

Clara N. Golhen-Mateo<sup>1</sup>, Carlos Galindo-Morata<sup>1</sup>, Pablo Galve<sup>1,2,3</sup>, Mojahed Abushawish<sup>1</sup>, Juan José Vaquero<sup>4,5</sup>, David Pérez-Benito<sup>4</sup>, Luis Batres<sup>4</sup>, Joaquin L. Herraiz<sup>1,2</sup>, Jose M. Udías<sup>1,2</sup>

<sup>1</sup>Grupo de Física Nuclear, EMFTEL & IPARCOS, Universidad Complutense de Madrid, CEI Moncloa, Madrid, Spain

<sup>4</sup>Departamento de Bioingeniería, Universidad Carlos III de Madrid

<sup>2</sup>Health Research Institute of the Hospital Clínico San Carlos (IdISSC), Madrid, Spain

<sup>5</sup>Instituto de Investigación Sanitaria Gregorio Marañón, Madrid

<sup>3</sup>Institute for Physical and Information Technologies “Leonardo Torres Quevedo”, ITEFI, Spanish National Research Council (CSIC), Madrid, Spain

cgolhen@ucm.es

Grupo de Física Nuclear @ UCM

## INTRODUCTION

Accurate interaction-vertex identification is essential for high-resolution PET [1].

Several detector configurations have been proposed:

- **Pixelated Crystal:** Achieves high XY resolution, but no DOI information.
- **Monolithic Crystal:** DOI information but limited XY resolution.
- **RETIMAGER Crystal (this work):** Crystals pixelated with laser-engraved semi-transparent walls enjoy the best properties of both extremes.

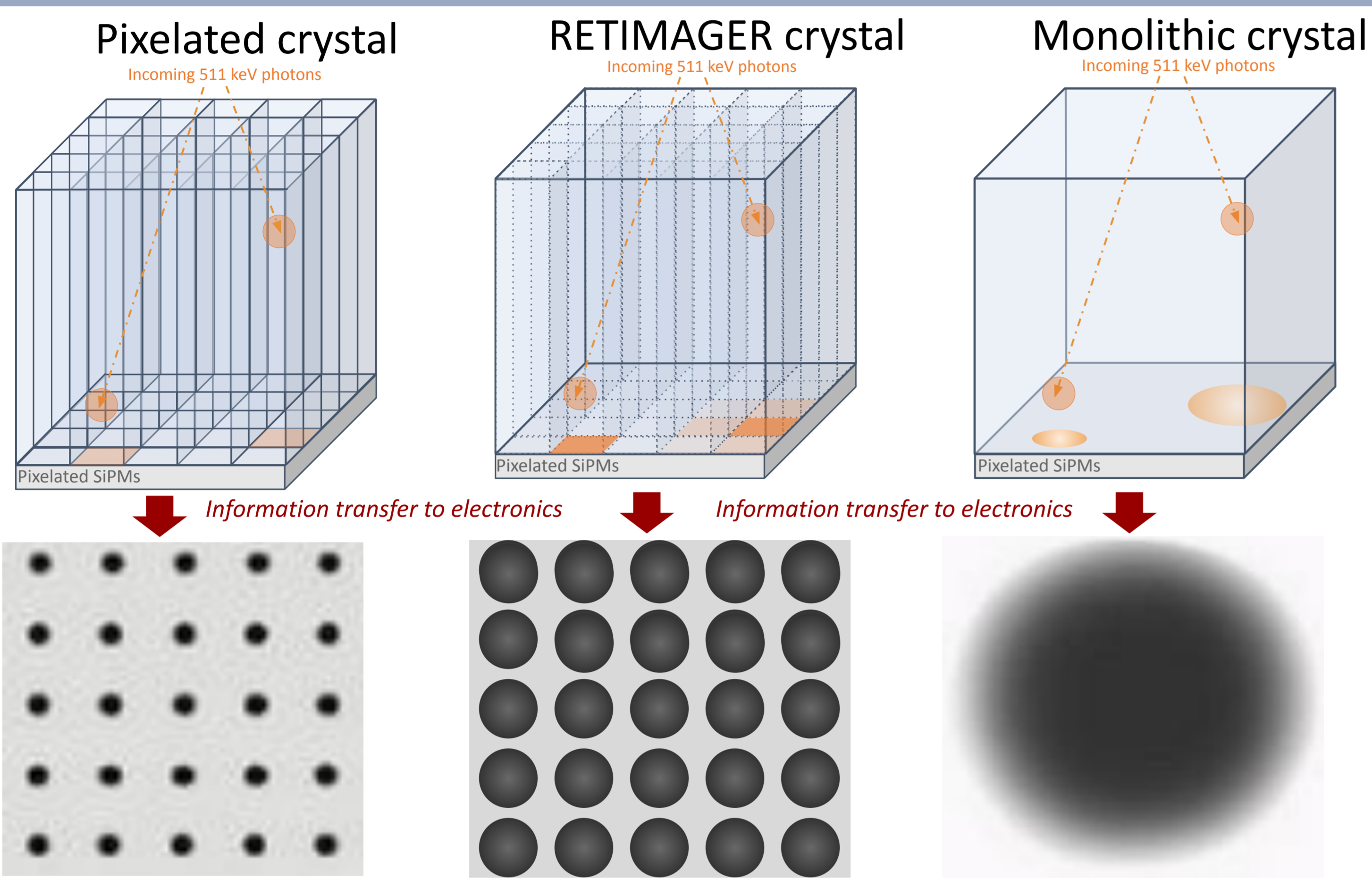


Fig. 1. Comparison between pixelated (left), monolithic (right) and our laser-engraved (center) scintillation crystals.

## METHODOLOGY

### A. Detector characteristics

- Prototype: 61 hexagonal SiPMs (2.16 mm) coupled to a laser-engraved hexagonal LYSO crystal block (17.6 mm side and 13 mm thickness).
- Simulations explore different pixel patterns and inter-pixel transparencies from 0 % to 100 % with ESR-coated or black lateral walls.

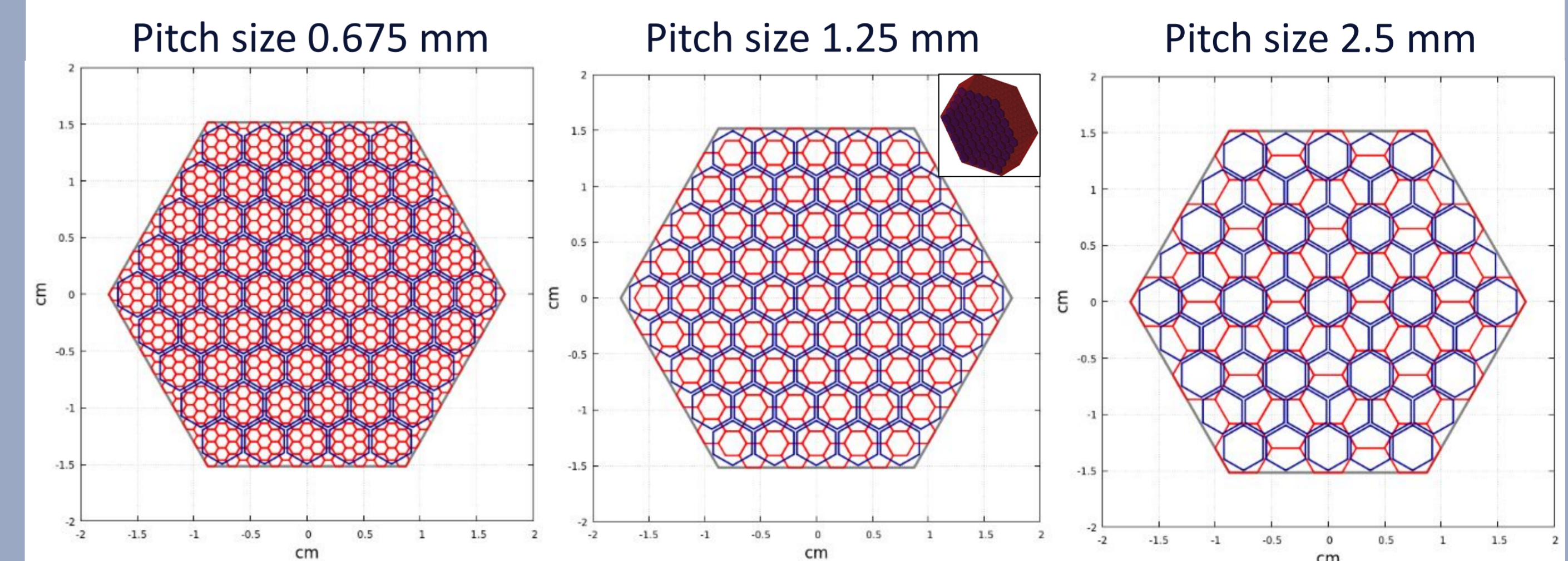


Fig. 2. Geometrical layouts of the detector block for three pixel sizes (side = 0.675 mm, 1.25 mm, and 2.5 mm) showing the correspondence between crystal pixels (red) and SiPMs (blue).

### B. GOSS simulations

Optical photon transport modeled with the GPU-based GOSS code, which simulates reflection, absorption, and detection to generate realistic SiPM light distributions for each geometry [4].

### C. Deep Learning algorithms

Neural networks trained on  $3 \cdot 10^5$  simulated events per simulated scenario to predict 3D interaction vertices and quantify XY/DOI errors.

## RESULTS

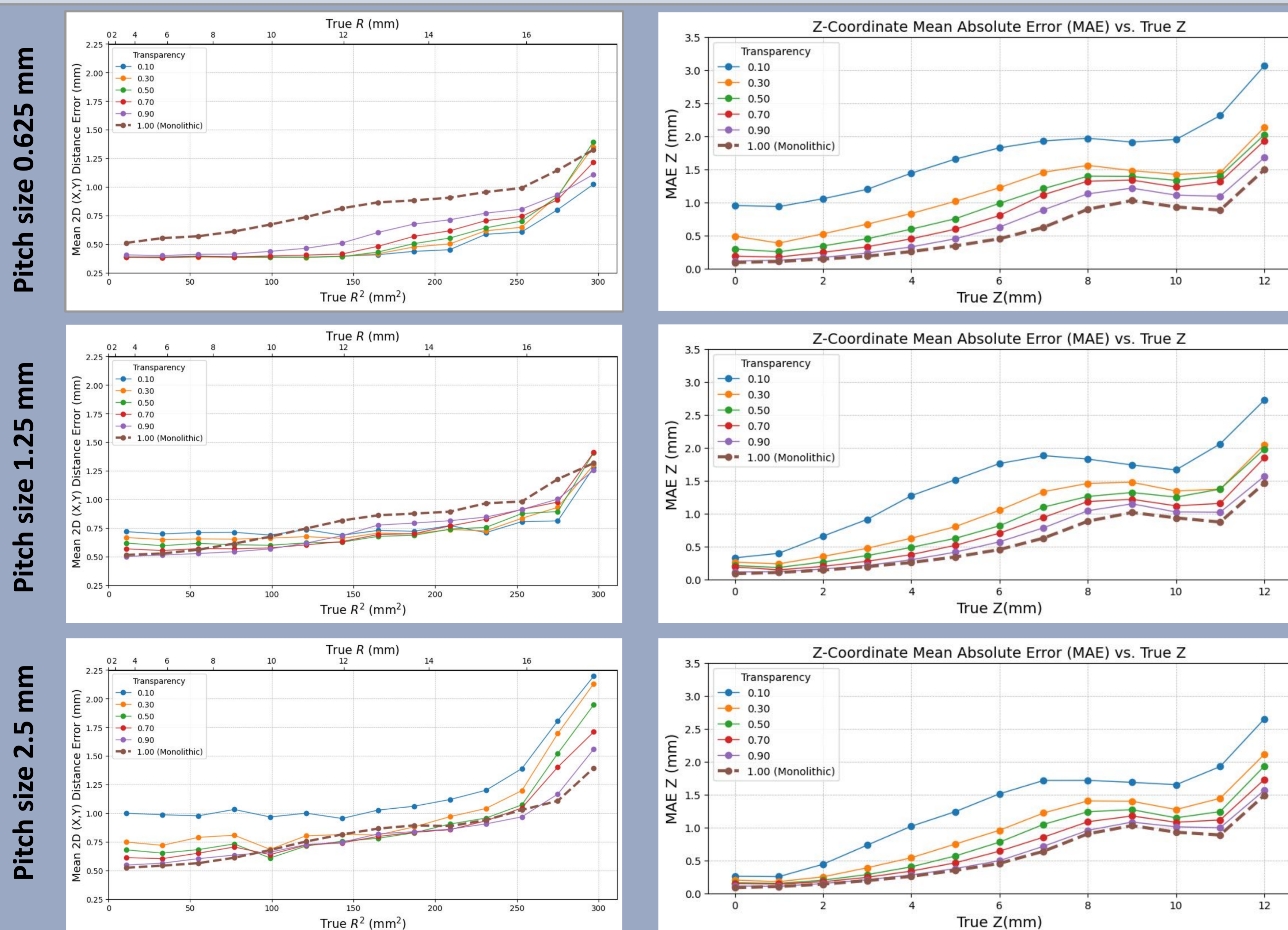


Fig. 3. XY-coordinate prediction error vs. true radius (top) and squared radius (bottom) on the left, and Mean Absolute Error (MAE) in Z vs. true depth on the right, for different transparencies and pitch sizes. Higher transparency and smaller pitches improve XY accuracy, with a slight decrease in DOI precision.

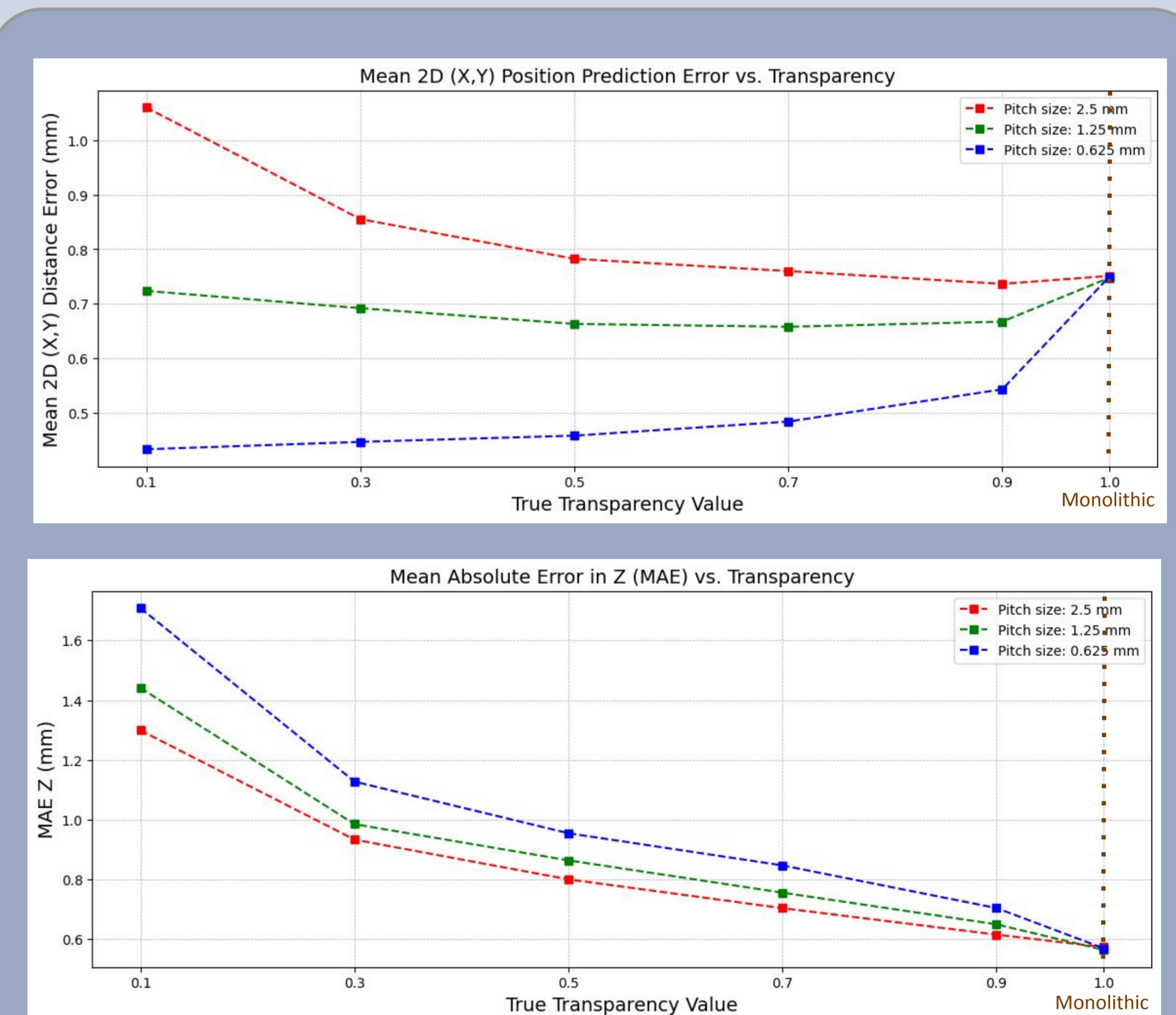


Fig. 4. Top: Mean 2D (XY) position prediction error versus transparency for different crystal pitch sizes. Position accuracy increases with higher transparency and smaller pitch, but for pitch sizes of 1.25 and 0.625 mm, semi-transparent walls outperform the monolithic case. Bottom: Mean Absolute Error (MAE) in Z versus transparency. Better performance is seen at higher transparencies at larger pitch sizes, reflecting improved DOI determination for the monolithic case.

## CONCLUSIONS

- Semi-transparent walls can outperform monolithic detectors in XY performance.
- DOI resolution with the proposed crystals was superior to pixelated configurations, only marginally worse than monolithic detectors.
- Positioning error in XY was smaller than 0.5 mm, and DOI was < 2 mm, not affected by the relatively large SiPMs (2.2 mm side) employed.
- These results demonstrate the potential advantage of semi-transparent walls for PET detectors.

## Acknowledgements

We acknowledge support from European Union as part of the European Innovation Council's Pathfinder Open Programme: RETIMAGER, 101099096; Spanish Government and Next GenerationEU Recovery and Resilience Facility (RRF) CPP 2021-008751 NEWMBI; Spanish Government and Next Generation EU/PRTR: DI2M: Smart detectors for molecular imaging (2021/C005/00147498); P. Galve acknowledges grant JDC2023-051754-I, funded by MCIU/AEI/10.13039/501100011033 and ESF+.

## References

- [1] W. W. Moses, "Fundamental limits of spatial resolution in PET," NIMA Accel. Spectrometers, Detect. Assoc. Equip., vol. 648, pp. S236–S240, Aug. 2011
- [2] E. Yoshida and T. Yamaya, "PET detectors with depth-of-interaction and time-of-flight capabilities," Radiol. Phys. Technol., no. 0123456789, Jun. 2024
- [3] Pérez-Benito, et al. (2019). SiPM-based PET detector module for a 4π span scanner. NIMA 936, 18–21.
- [4] Galve, P., et al. (2024, October). GOSS: GPU-based Optical Simulator of Scintillator Crystals. In 2024 IEEE NSS MIC RTS